I. Troch, F. Breitenecker, eds. ISBN 978-3-901608-35-3

MODELING AND SIMULATION OF THE DYNAMICS OF FUEL-CELL DRIVEN HYBRID POWERTRAINS

Markus Özbek, Dirk Söffker
University of Duisburg-Essen, Germany

Corresponding author: Dirk Söffker, Chair of Dynamics and Control, University of Duisburg-Essen, Lotharstr. 1-21, 47057 Duisburg, Germany, soeffker@uni-due.de

Abstract. In this contribution, modeling and simulation concepts of fuel cell-based hybrid powertrains for vehicles and other applications are presented. Mathematical models of fuel cells, DC/DC-converters, DC-Motor, and SuperCaps are put together and can simulate an arbitrarily load profile as well as a driving cycle for vehicles as a hybrid powertrain. The models are dynamical and, for the fuel cells, also include temperature effects. A Hardware-in-the-Loop test rig is built up, based on the models and results derived from these simulations and also shortly presented in this contribution. Further on, a power management algorithm is implemented and presented in the simulations. The power management shows a clear difference in the load gradients on the fuel cells, which are lower in presence of a power management. This increases the life time of the fuel cells. The simulation models shall complement the HiL test rig in order to give faster development time for future hybrid vehicle researches and power management developments.

1 Introduction

Fuel cells belong to one of the key technologies to overcome the future environmental challenges. Their benefits lie in their fast refuel (of hydrogen) time and, in contrast to conventional batteries, a high energy density. Combining the high energy density of hydrogen with the high energy flow rate of SuperCaps an energy efficient hybrid powertrain system can be realized. This is depicted in Figure 1. To understand the dynamics of such complex systems, simulation models serve as an important step in analysis and design of suitable topologies, control strategies, and power management to be used for the final design. The focus of this contribution is related to the models and simulation concepts. The implementation and validation of the developed methods with an Hardware-in-the-Loop (HiL) simulation test rig as depicted in Figure 3 is done but not detailed here.

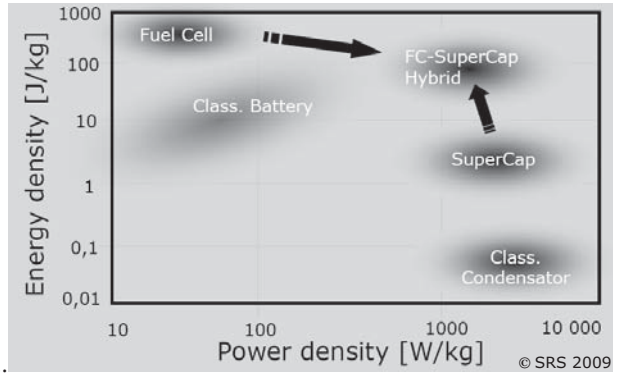

Figure 1: A combination between Fuel Cells and SuperCaps seems to be the optimal combination in a hybrid concept due to the high energy density of Fuel Cells and the high power density of SuperCaps

2 Component Modeling

An example how hardware and software models can interact is shown in Figure 2. A powertrain test rig, which is built based on the models of the outlined components and used for setting up different topologies and power management strategies is shown in Figure 3, where two three-phase permanent magnet synchronous electrical motors are mechanically connected and serve to simulate a fuel cell hybrid power train (drive motor) within a HiL-environment, which acts on the drive motor as external load (load motor). Components which interact with an environment can be replaced by models and simulated using a real-time processor, hence giving an economically favorable, safe, and experimentally realized simulation environment.

In the subchapters the modeling of the components in the HiL powertrain is described. The components include fuel cells, ultracapacitors, DC-motor, and DC/DC-converters.

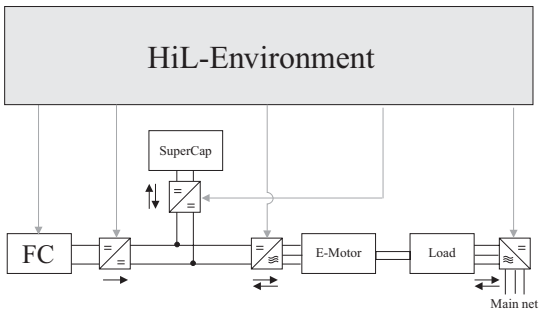

Figure 2: Structure of the HiL-concept using the introduced models

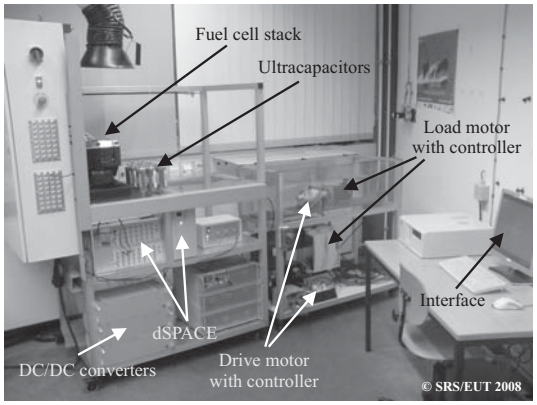

Figure 3: HiL test rig with the hardware components and the acquisition hardware, which realizes environmental load on the drive motor, the control concepts, and power management.

3 Fuel Cells

The fuel cell model used here, is based on the model developed in [4] and extended to consider temperature dynamics. The inputs to the fuel cell model are the voltages to the electrical motor in the air compressor and the cooling water pump respectively. Furthermore, in contrast to [4], the model is also extended to include a dynamic model of the compressor including its electrical motor. The electrical DC-motor model is presented in Chapter 3.2. The current, which is drawn from the fuel cells is regarded as a disturbance [4]. The outputs of the system are stack voltage U_{fc}, net power output P_{fc}, and excess oxygen ratio $O_{2,out} = \frac{\dot{m}_{fc,in}}{\dot{m}_{fc,reacted}}$, which is the ratio between the feeded air and the reacted air in the fuel cell stack. The anode and cathode inlet manifolds are regarded as a lumped model and in contrast to [4] the fuel cell stack temperature T_{fc}, is a dynamic variable depending on current, cooling water temperature, and inlet air and hydrogen temperatures.

3.1 SuperCaps

SuperCaps have a superior power density compared to fuel cells and batteries and hence are used in this hybrid concept to compensate for fast transient power demands. They differ from conventional batteries such that no chemical reactions occur and they have a very low inner resistance which explains the dense power outputs. The porous inner structure gives the ability to store a large amount of charge in comparison to conventional capacitors, while the behavior differs slightly. The output voltage is a nonlinear function of the charge, in contrast to conventional capacitors, and is regarded in the model. The SuperCaps behavior is modeled using analytical methods based on given approaches [6]. For the validation and for the test rig, SuperCaps with a size of 3000 Farad and a maximum voltage of 2.7 Volts per cell are used.

The progress how to model and identify the parameters is outlined in [6] and explained shortly here. First, the

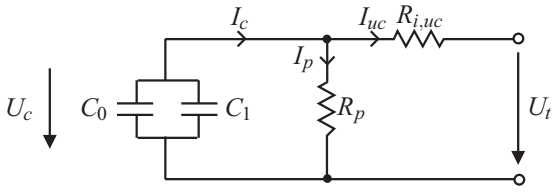

Figure 4: Schematic diagram of a supercapacitor model with variable capacitance

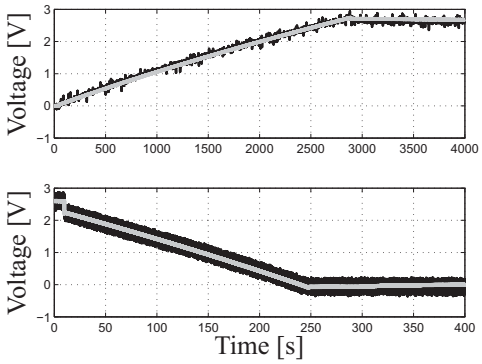

Figure 5: Validation of the ultracapacitor model. Above figure shows the charging with 3A and bottom figure shows discharging with 30A. Dark line - Measurement, Bright line - Simulation

inner resistance parameter $R_{i,uc}$, as depicted in Figure 4 is identified by discharging the SuperCaps with a high step current and then calculated as $R_{i,uc} = \frac{\Delta U_c}{\Delta I_c}$. The value was determined to $R_{i,uc} = 0.012$ Ohm. The variable capacitance, which varies continuously with the capacitor voltage U_c can be described as

$$C(U_c) = C_0 + C_1 U_c. \tag{1}$$

To identify the parameters C_0 and C_1, experiment tests on the SuperCaps are conducted. The equation (1) considers that the capacity is varying with the voltage according to $C(U_c) = \frac{dQ}{dU_c}|_{U'}$ for a given capacitor voltage U'. Integrating and solving for the total charge gives $Q = CU_c$ which is commonly known for conventional capacitors. Integrating the expression (1) with voltage gives

$$\int_0^{U_c} C(U_c) = Q = C_0 U_c + \frac{C_1 U_c^2}{2}. \tag{2}$$

Inserting $Q = CU_c$ in (2) gives the final expression of the equivalent capacitance for expressing the total charge in a SuperCap

$$C_q = C_0 + \frac{C_1 U_c}{2}. \tag{3}$$

With this expression inserted in Equation 1, the term C_1 can be identified by

$$C_1 = \frac{2}{U_c}(\frac{Q}{U_c} - C_0) = \frac{2}{U_c}(\frac{I_c(t_f - t_i)}{U_c} - C_0), \tag{4}$$

where t_i and t_f are the initial and final times for the test. The parameter C_0 is identified by inducing a constant current for a small time range and measure the voltage difference according to $C_0 = I_c \frac{\Delta t}{\Delta U_c}$. The constant is determined to $C_0 = 2600$. The capacitor voltage can then be described as

$$U_c = U_c^0 - \frac{1}{(C_0 + C_1 U_c)} \int I_c dt. \tag{5}$$

This gives the terminal voltage of the SuperCap

$$U_{t,uc} = U_c - R_{i,uc} I_{uc}, \tag{6}$$

where $R_{i,uc}$ is the internal resistance and I_{uc} is the main current to and from the SuperCap.

The validation of the model is depicted in Figure 5, where a constant current of 3A first charged the SuperCap and then being discharged with a 30A constant current.

3.2 Model of DC-Motor

The three-phase synchronous permanent magnet motor which is used in the application as drive motor, as well as in the air supply system of the fuel cell system are here modeled as DC-Motors.

The electrical diagram of the armature and the free body diagram of the rotor for the compressor DC-motor are shown in Figure 6. In this model, the compressor speed and the armature current are defined by two ordinary differential equations. According to the law of conservation of angular momentum the dynamic behavior of the compressor speed ω_{cp} is defined as

$$J_{cp} \frac{d\omega_{cp}}{dt} = \tau_{cm} - \tau_f - \tau_{cp}, \tag{7}$$

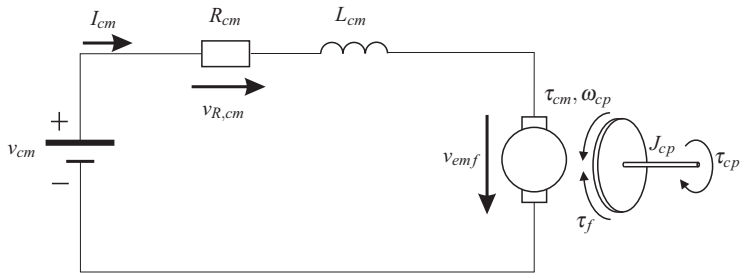

Figure 6: Schematic representation of the compressor DC-motor

where J_{cp} is the combined inertia of the compressor and the motor, τ_{cm} denotes the compressor motor torque, τ_{cp} expresses the external load on the motor, e.g. torque required to drive the compressor and τ_f stands for the torque loss in the motor because of friction. The part τ_{cp} is calculated by the second part of the compressor model. The dynamic behavior of the motor armature current I_{cm} is represented using the Kirchhoff's voltage law

$$L_{cm}\frac{dI_{cm}}{dt} = v_{cm} - v_{R,cm} - v_{emf}, \tag{8}$$

where L_{cm} is the electric inductance, v_{cm} the input voltage to the compressor motor, $v_{R,cm}$ the voltage drop through the internal electric resistance R_{cm}, and v_{emf} the induced voltage, i.e. the back electromotive force.

3.3 DC/DC converters

The main task of a DC/DC converter in a hybrid application, is to keep a constant output voltage despite of a varying input (supply) voltage for different loads, i.e. current outputs. It is an important task to control the output voltage to keep a constant value, especially for higher loads, low supply voltage, and fast transients. For some applications, it is desirable to control the output voltage to follow a reference signal and hence makes the DC/DC converter more complex and expensive. Another control variable could be the maximum current output that is allowed to be withdrawn. If higher currents are drawn then the voltage is rapidly decreased and hence the maximum output power is kept.

DC/DC converters are mainly categorized in three different types; buck, boost, and buck-boost converters. The buck converters reduce the output voltage in corresponding to the supply voltage and the boost converters increase the voltage output. The buck-boost converters can maintain the output voltage either in a higher or lower value to the supply voltage. Next, the buck and boost inverters, which are used in the hybrid system model for the drive motor, fuel cell system compressor motor, and as fuel cell output voltage converter are modeled and presented.

3.3.1 Boost DC/DC-converter

A boost converter is in this application used on the output voltage of the fuel cells. This gives a continuous bus voltage which is necessary for the drive motor to have a continuous supply voltage. The principles of a boost converter can be modeled according to Figure 7.

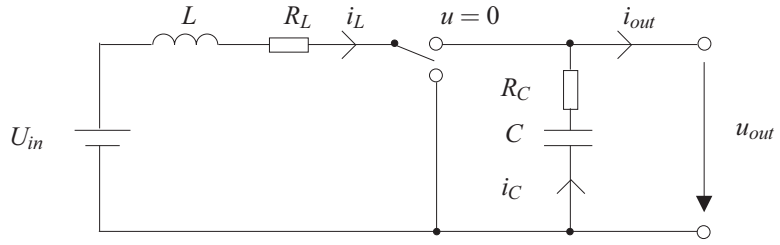

Figure 7: Boost DC/DC-converter

Energy losses are modeled with internal conductance and capacitance resistors R_L and R_C respectively. Applying Kirchhoff's law on the circuit yields the differential equations

$$\begin{aligned} u_{in} &= u_{\mathrm{L}} + u_{\mathrm{RL}} + u_{\mathrm{RC}} + u_C \\ u_{in} &= L\dot{i}_L + R_L i_L + (R_C i_C + \frac{1}{C}\int i_C)(1-u) \end{aligned} \tag{9}$$

or

$$u_{in} = L\dot{i}_L + R_L i_L + u_{out}, \tag{10}$$

with

$$i_L = i_C + i_{\text{out}} \tag{11}$$

and

$$u_{out} = U_{RL} + U_{RC}. \tag{12}$$

Boost converters are normally more difficult to control than buck converters. This is due to the point that boost converters are non-minimum phase systems [5]. Therefore, a continuous model is derived in the frequency domain. This decreases the complexity and the simulation time due to the lack of fast switching.

3.3.2 Continuous Boost DC/DC-converter

Due to the nonlinear output behavior of the fuel cell voltage, a boost-converter is inserted to boost the fuel cell voltage to a constant value. This converter is single-directional because the fuel cells cannot be loaded with recuperated energy. For simplicity and for decreasing the computational time in a simulation environment following transfer functions correspond to the DC/DC converter behavior:

From the common equation of a capacitor $\dot{U}_c C = I_c$ the bus voltage can be written as

$$U_{bus} = \frac{I_c}{sC} \tag{13}$$

in the Laplace domain. The inductive part of the DC/DC converter is separately controlled as in real DC/DC converters. This part consists of an inductor and an inner resistance for the losses as seen in Figure 8.

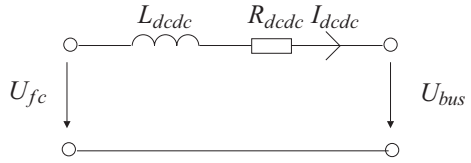

Figure 8: Inductive part of a boost DC/DC-converter

Deriving the equations gives

$$U_L + U_R = U_{fc} - DU_{bus}, \tag{14}$$

where D corresponds to the duty ratio of the switch shown in Figure 7. Rearranging and converting to the Laplace domain gives

$$I_{fc} = \frac{U_{fc} - DU_{bus}}{sL + R}. \tag{15}$$

3.3.3 Buck DC/DC-converter

The buck converter is inserted in the model as a DC-motor controller for speed. The buck converter can be modeled as shown in Figure 9. Buck converters are easier to control and hence a sliding mode control approach is applied.

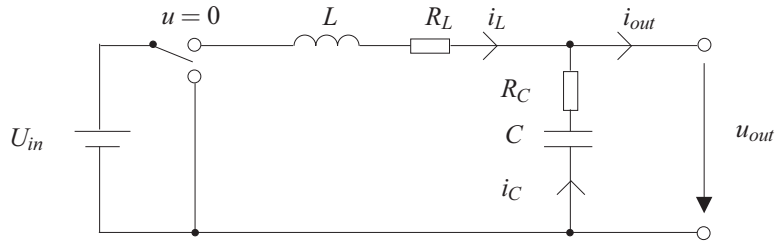

Figure 9: Buck DC/DC-converter

3.3.4 Sliding Mode Control

The sliding mode control determines the switching duty (value between 0 and 1) of the switch with the feedback of the inductance current i_L according to

$$u = \frac{1}{2}(1 - sign(S)), \tag{16}$$

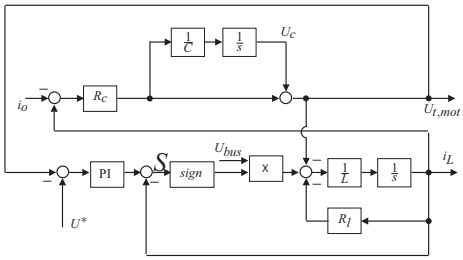

Figure 10: Model diagram of a buck-converter used as DC-motor controller with sliding mode control

where $S = i_L - i_L^*$. The switching allows building up current in the inductor and depending on the reference value of the output voltage, this current is released into the capacitor to give the desired output voltage. A block diagram with the model and controller is depicted in Figure 10. This switching causes ripples on the output voltage, which is common for all DC/DC converters and depends on the switching frequency which is set as constant. Consequently, a too high switching frequency slows the simulations and hence a compromise must be made between simulation speed and output voltage ripples. In order to guarantee stability of the sliding mode controller the requirement $S\dot{S} < 0$ must be fulfilled [1].

4 Hybrid Application

The question of which topology is the perfect one for a predefined given loadprofile and the required performance, is a key question for a successful hybrid application but not regarded here. In this paper, the so called series hybrid concept [2], depicted in Figure 11, will be used for simulating the models and implementing power management strategies. Using hybrid power sources overall helps decreasing fuel consumption and gives environmental benefits. A hybrid system is defined as having two or more power sources. In hybrid applications, an auxiliary power source is used to support the main source (combustion engine which drives a generator or like in this case fuel cells) with additional power. Depending on the topology, application, and power management, the beneficial features can be to track a reference value better, to increase the life time of the main power source, or to save fuel.

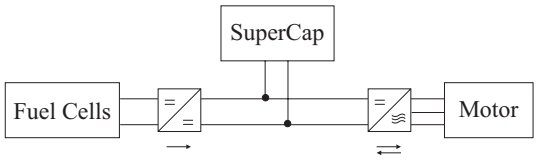

Figure 11: Series hybrid topology of the fuel cell powertrain for a hybrid vehicle

From Figure 12, the benefits of a hybrid system are clearly highlighted. The SuperCaps and Fuel Cell models are simulated separately for a power output step. It is seen how fast the dynamics of the SuperCaps are in comparison to the Fuel Cells and hence compensates for lack of dynamics in a hybrid system.

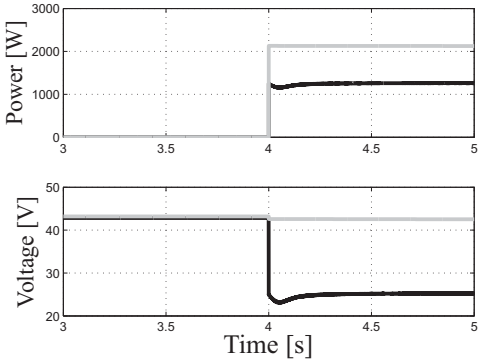

Figure 12: Simulation of a power step output on the SuperCap model and the Fuel cell model correspondingly. The faster dynamics of the SuperCaps is clearly seen. Dark Line - Fuel Cells, Bright Line - SuperCaps

4.1 Simulation Results and Power Management

The models derived in this paper are interconnected together and can simulate any load scenario applied on a hybrid system topology. A measured load profile is directly applied on the DC-motor model as a torque load,

the results are presented in Figure 13. The load profile corresponds to the dark line and includes recuperation movements. The SuperCaps are recuperating in negative power loads. The fuel cells are limited to 1.2kW load due to the limited number of cells.

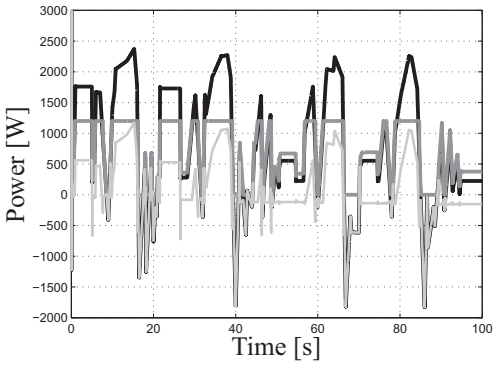

Figure 13: Simulation results for a given load profile. Dark Line - Power Electromotor, Grey Line - Power Fuel Cells, Bright Thin Line - Power SuperCaps

Additionally, a vehicle model is included in the hybrid model in order to simulate different driving scenarios. As a first scenario an acceleration-deceleration drive-cycle of the vehicle to prove the model interactions and to make plausibility checks is used. The vehicle accelerates to 54km/h at time 10s and decelerates back to standstill at time 25s.

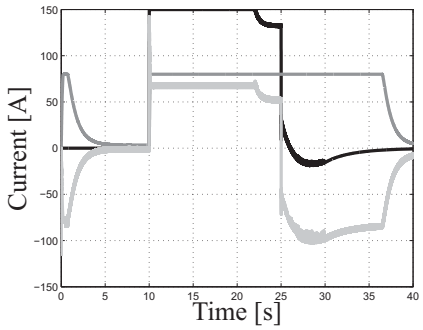

Figure 14: Current flows between fuel cell, ultracapacitor, and motor, during a acceleration-deceleration cycle. Dark line - Motor current, Gray line - Fuel Cell current, Bright line - Ultracapacitor current

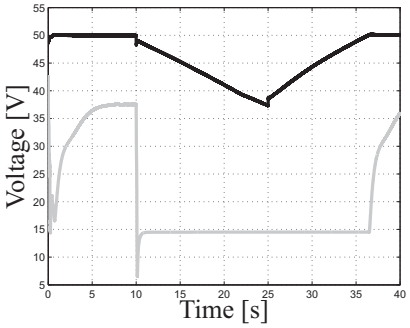

Figure 15: Voltage change for bus voltage and fuel cell during a acceleration-deceleration cycle, Dark line - Bus voltage, Bright line - Fuel Cell voltage

The results are presented in Figure 14 and 15, where voltage outputs and current flows between the modeled components are depicted. Initially, the DC/DC converter has a reference value to hold 50V on at the bus voltage. The ultracapacitors are charged to 48.6V and hence are overcharged with a sudden current flow from the fuel cells as can be seen in the first 3-4 seconds in Figure 14. This implies to a short-circuit current and can be very large, due to the low internal resistance of ultracapacitors, if the potential differences are too large. Between 10 and 25s, a step input is given to the vehicle and it starts to accelerate. The motor current is limited to 150A, which is based on the BLDC motor used on the HiL test rig, and the fuel cell current to 80A which is assumed as the maximum

current the real fuel cell stack is limited to. From this time interval the benefits of a hybrid concept are clearly seen as the motor is provided current from the fuel cell and the ultracapacitor at the same time. During this period, the system works on its maximum and the ultracapacitor is depleted with charge which causes the bus voltage to decrease as can be seen in Figure 15. At about 23-25s, the bus voltage decreases below the terminal voltage of the DC-motor and hence the small decrease in current and dynamics. After 25s the vehicle decelerates and it is clearly seen how a negative motor current (charge current) is produced from regenerative braking and fills the ultracapacitor, which emphasizes the benefits of hybrid systems.

4.1.1 Power Management

As an example of power management used in this application, the SuperCaps state-of-charge (SOC) is kept at a constant level for three reasons:

1) to optimize the ability of receiving regenerated power (it is optimal to keep the SOC as close to the maximum efficiency level as possible),
2) not to waste an unpredictable regenerative breaking due to fully charged SuperCaps. To keep the SuperCaps fully charged would mean a waste of regenerative power in a heat sink in order not to damage the SuperCaps due to over charging, and
3) to guarantee available power during sudden power peak demands.

The size of the SuperCap bank is already determined and presented in [3]. For the used topology, two different simulations were conducted. The first used a non-controllable DC/DC-converter with output voltage of 42V and the second simulation included a DC/DC-converter with implementable power management strategies by controlling the maximum allowed output current I_{max}. In order to guarantee the three outlined goals for an arbitrary load profile means the SuperCap capacity size must be indefinitely large. Therefore, compromises must be made. These compromises are set depending on the given load profile. A power management strategy has the task to distribute the available power between the components. When the vehicle power demand exceeds the available stored power, it must guarantee system stability and comfortability for the user and at the same time regard that no damages occur to the energy sources. As example the power distribution between fuel cells and SuperCaps is calculated by choosing the actual SOC of the SuperCaps and split the power proportionally according to the rule

$$I_{max} = (1 - SOC) I_{maxdcdc}, \tag{17}$$

where $I_{maxdcdc}$ denotes the overall possible maximum current that can be withdrawn from the DC/DC-converters. In this case $I_{maxdcdc}$ is set to 35 A, based on an existing DC/DC-converter available on the HiL test rig, which is the subject for this contribution.

The results are presented in Figure 16. The difference between the power output of the fuel cells with and without power management is clearly seen. The high peaks and dynamics of the output power for the fuel cells highly decrease the life time of the fuel cells due to their sensitivity towards current-, temperature-, and humidity-gradients. When implementing power management the output power of the fuel cells becomes more smooth and with lower gradients and hence, increases the life time of the fuel cells.

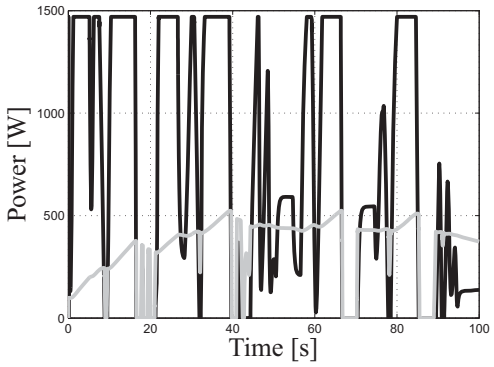

Figure 16: Difference in Fuel Cell power output with a simple power management and without power management. The softer and more continuous output is preferable for increasing life time of the Fuel Cells. Dark line - without power management, Bright line - with power management

5 Conclusion

Modeling of components as well as the related full system design model of fuel cell-based hybrid powertrain systems and applications were presented. A fuel cell model, a SuperCap model which also was validated, a buck DC/DC-converter which is used as a DC-motor controller, its corresponding DC-motor, and an equivalent model of a boost DC/DC converter are developed and presented. The models were set up in a defined topology with suitable inputs and outputs between the sub-models to serve as a future platform for analysis and simulation of fuel cell driven hybrid concepts. A powertrain of a smaller vehicle was implemented in the modeling concept to simulate a simple driving cycle for smaller vehicles.

6 References

[1] C. Edwards and K.S Sarah: *Sliding Mode Control - Theory and Applications*. Taylor & Francis, Padstow, UK, 1998.

[2] A. Emadi, K. Rajashekara, S. S. Williamson and S. M. Lukic: *Topological Overview of Hybrid Electric and Fuel Cell Vehicular Power System Architectures and Configurations*. IEEE Trans. on Vehicular Technology, 54 (2005), 763–770.

[3] M. Özbek and D. Söffker: *Hardware-in-the-loop-based simulation of a fuel cell-driven powertrain System - Conception, Modeling, and Simulation Results*. In: Proc. MOVIC08, München, Germany, 15-18 Sept. 2008.

[4] J. T. Pukrushpan, A. G. Stefanopoulou and H. Peng: *Control of Fuel Cell Power Systems: Principles, Modelling, Analysis and Feedback Design*. Springer-Verlag, Bangkok, Thailand, 2004.

[5] R. Venkataramana, A. Sabanovic and S. Cuk: *Sliding Mode Control of DC-DC Converters*. In: Proc. of IECONŠ85, San Francisco, USA, 1985.

[6] L. Zubieta and R. Bonert: *Characterization of Double-Layer Capacitors for Power Electronics Applications*. IEEE Trans. on Industry Applications, 36 (2000), 199–204.